# Molecularly Specific Studies of the Frictional Properties of Monolayer Films: A Systematic Comparison of $CF_3$-, $(CH_3)_2CH$-, and $CH_3$-Terminated Films

Hyun I. Kim, Michael Graupe, Olugbenga Oloba, Thomas Koini, Syed Imaduddin, T. Randall Lee,* and Scott S. Perry*

*Department of Chemistry, University of Houston, Houston, Texas 77204-5641*

*Received October 23, 1998. In Final Form: February 12, 1999*

The origin of frictional forces in self-assembled monolayers (SAMs) was investigated through systematic correlation of the frictional properties with the chemical structure/composition of the films. Atomic force microscopy was used to probe the frictional properties of the SAMs formed by the adsorption of methyl-, isopropyl-, and trifluoromethyl-terminated alkanethiols on Au(111) surfaces. The frictional properties of mixed monolayers composed of varying concentrations of the methyl- and trifluoromethyl-terminated thiols were also studied. Polarization modulation infrared reflection adsorption spectroscopy was used to measure the vibrational spectra of each of these monolayers and in turn to determine that each was characterized by a well-packed backbone structure. For these films, which differed only in the nature of the outermost chemical functionality, a substantial enhancement in the frictional response was observed for films with isopropyl- and trifluoromethyl-terminal groups and for mixed monolayers containing small concentrations of the trifluoromethyl-terminated component. These results strongly support the model that the difference in friction in such systems arises predominantly from the difference in the size of the terminal groups. Larger terminal groups in films of the same lattice spacing give rise to increased steric interactions that provide pathways for energy dissipation during sliding.

## Introduction

Organic thin films have found use in a wide range of technological applications. One area of particular interest is the use of lubricating organic layers for the control of friction and wear. As the trend toward miniaturization in device fabrication continues, protecting and lubricating films having molecular scale dimensions are now being targeted. Examples include the application of monomolecular layers of polyperfluoroethers on the surface of hard disk drives[1] and the potential use of self-assembled monolayers (SAMs) for the lubrication of newly emerging microelectronic machines (MEMs).[2] As the thickness of lubricating layers in such applications approaches the monolayer regime, molecular properties such as composition, structure, and reactivity and their relation to friction and the prevention of wear become critical parameters in the overall performance of the system. As a result, many recent studies have sought to correlate frictional properties with the molecular details of thin organic films. These studies have used instrumentation such as the atomic force microscope (AFM),[3−9] the surface forces apparatus (SFA),[10−13] and the interfacial force microscope (IFM)[14] to measure interfacial forces on molecular dimensions.

In previous work with AFM, we explored the frictional properties of SAMs in which the chemical composition of the terminal end group of the organic monolayer was systematically varied.[8,9] Specifically, we formed SAMs on Au(111) from two distinct straight chain alkanethiols composed of 13 carbon atoms—one being fully hydrogenated and the other containing a hydrogenated backbone but terminated with a trifluoromethyl group. These studies sought to unravel the origin of the enhanced frictional properties of fluorinated organic films[15−21] by holding constant the structure and packing of the films while systematically introducing fluorine selectively to the region of the sliding interface. Upon the introduction of fluorine, we observed a 3-fold increase in friction as measured by AFM and attributed the increase to the relatively large size of fluorine vs hydrogen atoms. We postulated that the introduction of fluorine leads to

(1) Homola, A. M.; Mate, C. M.; Street, G. B. *MRS Bull.* **1990**, *15*, 45.
(2) Deng, K.; Collins, R. J.; Mehregany, M.; Sukenik, C. N. *J. Electrochem. Soc.* **1995**, *142*, 1278.
(3) Lemieux, M.; Hazel, J.; Shevchenko, V. V.; Klimenko, N.; Sheludko, E.; Tsukruk, V. V. *Polym. Prepr.* **1998**, *39*, 1181.
(4) Tsukruk, V. V.; Bliznyuk, V. N. *Langmuir* **1998**, *14*, 446.
(5) Mate, C. M.; McClelland, G. M.; Erlandsson, R. Chiang, S. *Phys Rev. Lett.* **1987**, *59*, 1942
(6) Carpick, R. W.; Agrait, N.; Ogletree, D. F.; Salmeron, M. *J. Vac. Sci. Technol. B* **1996**, *14*, 1289.
(7) Xiao, X.; Hu, J.; Charych, D. H.; Salmeron, M. *Langmuir* **1996**, *12*, 235.
(8) Kim, H. I.; Koini, T.; Lee, T. R.; Perry, S. S. *Langmuir* **1997**, *13*, 7192.
(9) Kim, H. I.; Koini, T.; Lee, T. R.; Perry, S. S. *Tribol. Lett.* **1998**, *4*, 137.
(10) Israelachvili, J. N.; McGuiggan, P. M.; Homola, A. M. *Science* **1988**, *240*, 189.
(11) Yamada S.; Israelachvili, J. *J. Phys. Chem. B* **1998**, *102*, 234.
(12) Reiter, G.; Demirel, A. L.; Granick, S. *Science* **1994**, *263*, 1741.
(13) Van Alsten, J.; Granick, S. *Langmuir* **1990**, *6*, 876.
(14) Thomas, R. C.; Tangyunyong, P.; Houston, J. E.; Michalske, T. A.; Crooks, R. M. *J. Phys. Chem.* **1994**, *98*, 4493.
(15) Meyer, E.; Overney, R.; Lüthi, R.; Brodbeck, D.; Howald, L.; Frommer, J.; Güntherodt, H.-J.; Wolter, O.; Fujihira, M.; Takano, H.; Gotoh, Y. *Thin Solid Films* **1992**, *220*, 132.
(16) Overney, R.; Meyer, E.; Frommer, J.; Brodbeck, D.; Howald, L.; Güntherodt, H.-J.; Fujihira, M.; Takano, H.; Gotoh, Y. *Nature* **1992**, *359*, 133.
(17) Overney, R. M.; Meyer, E.; Frommer, J.; Güntherodt, H.-J.; Fujihira, M.; Takano, H.; Gotoh, Y. *Langmuir* **1994**, *10*, 1281.
(18) Levine, O.; Zisman, W. A. *J. Phys. Chem.* **1957**, *61*, 1068.
(19) Briscoe, B. J.; Evans, D. C. B. *Proc. R. Soc. London, A* **1982**, *380*, 389.
(20) DePalma, V.; Tillman, N. *Langmuir* **1989**, *5*, 868.
(21) Chaudhury, M. K.; Owen, M. J. *Langmuir* **1993**, *9*, 29.

10.1021/la981497h CCC: $18.00 
Published on Web 04/08/1999

**Scheme 1**

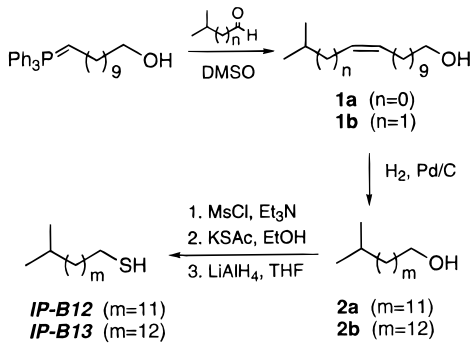


enhanced intra- and intermolecular steric interactions for the $CF_3$-terminated films.

The present study represents a further extension of this research with a focus on the influence of steric interactions upon the interfacial frictional properties. As before, this study employs AFM to measure the structural (molecular spacing) and frictional properties of well-ordered alkanethiols adsorbed on Au(111). Specifically, we examined the frictional properties of mixed SAMs composed of $CH_3$- and $CF_3$-terminated alkanethiols having the same chain lengths (for both odd and even numbers of carbon atoms). We compared the frictional properties of these mixed SAMs to those of the previously reported single-component SAMs.[8] We also explored the frictional properties of SAMs terminated with sterically large isopropyl moieties. In all systems examined, the incorporation of a large terminal group into the SAMs led to a substantial increase in the frictional response of the films.

## Experimental Section

**Nomenclature.** For simplicity, we denote the names of the alkanethiols as follows: tridecanethiol ($CH_3(CH_2)_{12}SH$), **H1-B12**; tetradecanethiol ($CH_3(CH_2)_{13}SH$), **H1-B13**; hexadecanethiol ($CH_3(CH_2)_{15}SH$), **H1-B15**; 13,13,13-trifluorotridecanethiol ($CF_3$-$(CH_2)_{12}SH$), **F1-B12**, 14,14,14-trifluorotetradecanethiol ($CF_3$-$(CH_2)_{13}SH$), **F1-B13**; 16,16,16-trifluorohexadecanethiol ($CF_3$-$(CH_2)_{15}SH$), **F1-B15**; 13-methyltetradecanethiol ($((CH_3)_2CH$-$(CH_2)_{12}SH$), **IP-B12**; and 14-methylpentadecanethiol ($((CH_3)_2CH$-$(CH_2)_{13}SH$), **IP-B13**. The prefix indicates the chemical composition of the terminal group: **H1** denotes methyl, **F1** denotes trifluoromethyl, and **IP** denotes isopropyl. The number following the letter "**B**" indicates the number of carbon atoms in the backbone of the chain (i.e., the number of methylene groups between the mercapto group and the terminal functional group).

**Materials.** The normal alkanethiols, 11-bromoundecanol, triphenylphosphine, methanesulfonyl chloride, isovaleraldehyde, and isobutyraldehyde were obtained from Aldrich Chemical Co. and used as received. DMSO (Aldrich Chemical Co.) was dried and distilled over calcium hydride under vacuum. THF (EM Science) was dried by passage through alumina. Acetonitrile (anhydrous), hexane, diethyl ether, and triethylamine were used as received from EM Science. Silica gel (Fisher, 60−200 mesh) was used for column chromatography. Nuclear magnetic resonance (NMR) spectra were collected on a General Electric QE−300 spectrometer operating at a resonance frequency of 300 MHz for $^1H$ and 75 MHz for $^{13}C$. The trifluoromethyl-terminated alkanethiols were prepared as described previously.[22] Scheme 1 illustrates the preparation of the isopropyl-terminated alkanethiols, **IP-B12** and **IP-B13**.

**General Procedure for the Synthesis of 13-Methyltetradec-11-enol (1a) and14-Methylpentadec-11-enol (1b).** 11-Bromoundecanol (2.44 g; 9.71 mmol) and triphenylphosphine (2.55 g; 9.71 mmol) were dissolved in 50 mL of acetonitrile under argon and heated under reflux for 36 h. After cooling, the solvent was evaporated under vacuum. Dry DMSO (10 mL) was placed in a 100 mL round-bottomed flask. Under argon, 0.6 g of sodium hydride (15 mmol, 60% dispersion in mineral oil) was added, and the mixture was warmed to 60 °C until the evolution of hydrogen ceased. After the mixture was allowed to cool to 40 °C, the phosphonium salt (dissolved in 10 mL of DMSO) was added. The mixture was stirred at 40 °C for 1 h, and then 9.71 mmol of the aldehyde (0.88 mL of isobutyraldehyde or 1.05 mL of isovaleraldehyde) was added. After the mixture was stirred overnight at 40 °C, 50 mL of water was added, and the resulting mixture was extracted with diethyl ether (3 × 100 mL). The combined organic layers were washed with water (100 mL) and brine (100 mL), dried with magnesium sulfate, and evaporated to dryness under vacuum. The residue was redissolved in 300 mL of hexane and washed with acetonitrile (3 × 20 mL) to remove the triphenylphosphine oxide. The hexane layer was evaporated, and the crude product was purified by chromatography on silica gel using hexane/diethyl ether (3:1) as the eluent. 13-Methyltetradec-11-enol (**1a**) was obtained in 70% yield. $^1H$ NMR (300 MHz, $CDCl_3$): $\delta$ 5.25−5.13 (m, 2 H), 3.62 (t, $J$ = 6.6 Hz, 2 H), 2.58 (m, 1 H), 2.03 (q, $J$ = 6.3 Hz, 2 H), 1.60−1.48 (m, 3 H), 1.38−1.22 (m, 14 H), 0.88 (d, $J$ = 6.6 Hz, 6 H). 14-Methylpentadec-11-enol (**1b**) was obtained in 75% yield. $^1H$ NMR (300 MHz, $CDCl_3$): $\delta$ 5.43−5.30 (m, 2 H), 3.62 (t, $J$ = 6.6 Hz, 2 H), 1.99 (q, $J$ = 6.3 Hz, 2 H), 1.90 (t, $J$ = 6.3 Hz, 2 H), 1.64−1.50 (m, 4 H), 1.38−1.22 (m, 14 H), 0.82 (d, $J$ = 6.6 Hz, 6 H).

**General Procedure for the Synthesis of 13-Methyltetradecanol (2a) and 14-Methylpentadecanol (2b).** Palladium on carbon (0.20 g; 5% palladium) was suspended in 200 mL of hexane and stirred under an atmosphere of hydrogen for 30 min. The olefin (7.32 mmol) was dissolved in 20 mL of hexane and added to the catalyst suspension. Stirring under hydrogen was continued for 6 h. The reaction mixture was then filtered through a small pad of Celite. The filtrate was evaporated, giving the saturated alcohol in quantitative yield. 13-Methyltetradecanol (**2a**). $^1H$ NMR (300 MHz, $CDCl_3$): $\delta$ 3.62 (t, $J$ = 6.3 Hz, 2 H), 1.59−1.43 (m, 4 H), 1.37−1.10 (m, 20 H), 0.83 (d, $J$ = 6.6 Hz, 6 H). 14-Methylpentadecanol (**2b**). $^1H$ NMR (300 MHz, $CDCl_3$): $\delta$ 3.63 (t, $J$ = 6.3 Hz, 2 H), 1.60−1.43 (m, 4 H), 1.37−1.10 (m, 22 H), 0.83 (d, $J$ = 6.6 Hz, 6 H).

**General Procedure for the Synthesis of 13-Methyltetradecanethiol (IP-B12) and 14-Methylpentadecanethiol (IP-B13).** To a stirred solution of 7.32 mmol of the alcohol in 200 mL of hexane were added 3.06 mL (22.0 mmol) of triethylamine and 1.13 mL (14.6 mmol) of methanesulfonyl chloride at room temperature. After the mixture was stirred for 2 h, 100 mL of water was added. The layers were separated, and the aqueous layer was extracted with hexane (2 × 50 mL). The combined hexane layers were washed twice with 100 mL of water, dried with magnesium sulfate, and evaporated to dryness. The crude mesylate was dissolved in 100 mL of ethanol. Potassium thioacetate (2.51 g; 22.0 mmol) was added under argon, and the stirred mixture was warmed to 60 °C for 6 h. Water (100 mL) was added, and the mixture was extracted with hexane (3 × 100 mL). The combined hexane layers were washed twice with 100 mL of water, dried with magnesium sulfate, and evaporated to dryness. The crude alkyl thioacetate was dissolved in 50 mL of dry THF, and the solution was added slowly under argon to a slurry of 0.5 g (13.2 mmol) of lithium aluminum hydride (LAH) in THF at room temperature. The reaction mixture was refluxed under argon for 2 h. After the reaction was cooled, the excess LAH was destroyed by the dropwise addition of water. The mixture was acidified with 10% HCl until all precipitates were dissolved and then extracted with hexane (3 × 100 mL). The combined hexane layers were washed twice with 100 mL of water, dried with magnesium sulfate, and evaporated to dryness. The residue was purified by chromatography on silica gel using hexane as the eluent. 13-Methyltetradecanethiol (**IP-B12**) was obtained in 57% yield. $^1H$ NMR (300 MHz, $CDCl_3$): $\delta$ 2.50 (q, $J$ = 7.2 Hz, 2 H), 1.64−1.43 (m, 3 H), 1.38−1.10 (m, 21 H), 0.85 (d, $J$ = 6.6 Hz, 6 H). $^{13}C$ NMR (75 MHz, $CDCl_3$): $\delta$ 39.04, 34.03, 29.91, 29.68, 29.63, 29.57, 29.50, 29.05, 28.36, 27.95, 27.39, 24.62, 22.62. Anal. Calcd for $C_{16}H_{34}S$: C, 73.69; H, 13.19. Found: C, 74.18; H, 12.93. 14-Methylpentadecanethiol (**IP-B13**) was obtained in 58% yield. $^1H$ NMR (300 MHz, $CDCl_3$): $\delta$ 2.50 (q, $J$ = 7.2 Hz, 2 H), 1.66−1.43 (m, 3 H), 1.40−1.10 (m, 23 H), 0.85 (d, $J$ = 6.6 Hz, 6

(22) Graupe, M.; Koini, T.; Wang, V. Y.; Nassif, G. M.; Colorado, R., Jr.; Villazana, R. J.; Dong, H.; Miura, Y. F.; Shmakova, O. E.; Lee, T. R. *J. Fluorine Chem.* **1993**, *93*, 107.

H). $^{13}C$ NMR (75 MHz, $CDCl_3$): $\delta$ 39.03, 34.03, 29.92, 29.64, 29.58, 29.50, 29.05, 28.36, 27.94, 27.39, 24.61, 22.62. Anal. Calcd for $C_{16}H_{34}S$: C, 74.34; H, 13.26. Found: C, 74.01; H, 12.89.

SAMs were prepared by exposure of gold substrates containing (111) terraces to 1 mM solutions of the alkanethiols in ethanol for 24 h. The gold substrates were prepared by annealing a gold wire in a $H_2/O_2$ flame followed by rinsing with distilled water. AFM images and measurements were collected using a custom built head that consists of a single tube scanner and an optical deflection detection scheme. Data acquisition, control of the microscope head, image processing, and data analysis were carried out using RHK STM 100 control electronics and RHK SPM32 4.0 software. The laser diode signal was controlled and processed using RHK AFM 100 control electronics. Microfabricated $Si_3N_4$ cantilever assemblies (Digital Instruments) were used for imaging and friction measurements. The sharpness of the tips was routinely measured by imaging a reconstructed $SrTiO_3$ standard.[23] Values for the normal force constants and lateral force constants were estimated by modeling the bending and torsion of a triangular lever assembly and accounting for the specific shape and dimensionality of the lever assemblies as measured by TEM. Friction−load maps were collected in a number of areas on each sample according to procedures described in a previous publication.[24] To permit valid comparisons, the same AFM tip was used for all samples compared on a given plot.

Additional characterization of the structure and composition of the SAMs included X-ray photoelectron spectroscopy (XPS) and polarization modulation infrared reflection absorption spectroscopy (PM-IRRAS).[25] XPS spectra were collected with a PHI 5750 XPS system using a PHI 10-420 toroidal monochromator and a PHI 10-360 hemisperical analyzer. The monochromatic Al source (1486.6 eV) was operated at 350 W, and spectra were collected using a pass energy of 50 eV. The use of the monochromatic X-ray source minimized the degree of degradation of the C−F species during irradiation. PM-IRRAS spectra were collected using a Nicolet MAGNA-IR 860 Fourier transform spectrometer equipped with a liquid nitrogen-cooled mercury−cadmium−telluride (MCT) detector and a Hinds Instruments PEM-90 photoelastic modulator. The infrared light was incident upon the sample surface at 80°. With the polarization modulation approach, the polarization of the incident light was modulated between s- and p-orientations at a frequency of 37 kHz. A lock-in amplifier was used to detect simultaneously signals generated from each polarization. From these signals, the differential surface reflectivity ($\Delta R/R$) was calculated as the ratio $(R_p - R_s)/(R_p + R_s)$, where $R_p$ and $R_s$ represent the reflected signals for the respective polarizations. The data were collected for 1000 scans at a spectral resolution of 4 $cm^{-1}$ from SAMs prepared on silicon wafers that were coated first with chromium (ca. 100 Å) and then with gold (ca. 1000 Å).

## Results

**Mixed Monolayers of Methyl- and Trifluoromethyl-Terminated Alkanethiols.** Mixed monolayers of **H1-B12** and **F1-B12** self-assembled on gold substrates were prepared by adsorption from solutions of varying relative concentrations of the two alkanethiols. Similar mixed films were also prepared from solutions of **H1-B15** and **F1-B15**. Using this approach, two-component mixed self-assembled films were created in which the backbone structure of the films was held constant; only the surface concentration of the terminal groups was varied.

The choice of solvent used in the formation of SAMs is known to influence the relative adsorption rates of mixtures of alkanethiols.[26] We thus wished to establish the nature of any difference between solution and surface composition in the adsorption of the mixtures of alkanethiols under consideration here. The surface composition of the mixed monolayers was determined from measurements by XPS. The procedure involved the measurement of the C 1s, F 1s, and Au 4f core level spectra for monolayers of mixed composition. Figure 1 displays the spectra obtained from the 100% **F1-B15** film. A single peak (690.0 eV) was observed in the F 1s region while two distinct peaks (284.5 and 292.6 eV) were observed in the C 1s region for films containing the trifluoromethyl component. We assign the predominant peak at 284.5 eV to the carbon of the backbone chain and the peak at 292.6 eV to the terminal carbon of the trifluoromethyl group.[27] No other features were observed in any of the spectra measured for different surface compositions or for different chain lengths; only the intensities of the features associated with the presence of fluorine were observed to change. The mole fraction of the partially fluorinated component was determined from calculations using the integrated intensities of the F 1s peak and the Au 4f peaks of the underlying substrate. For these calculations, the ratio of the relative integrated intensities of these two regions obtained from the film synthesized from a 100% trifluoromethyl-terminated film was assigned as the end point

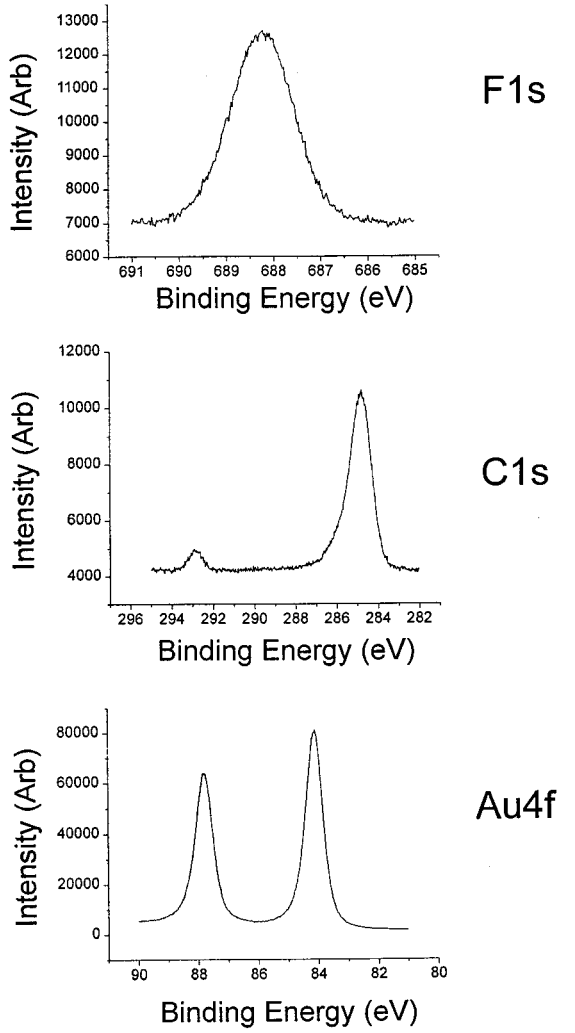


**Figure 1.** X-ray photoelectron spectra obtained from the F 1s, C 1s, and Au 4f regions for a self-assembled monolayer of 16,16,16-trifluorohexadecanethiol on Au(111).

(23) Sheiko, S. S.; Moller, M.; Reavekamp, E. M. C. M.; Zandbergen, H. W. *Phys Rev. B* **1993**, *48*, 5765.
(24) Perry, S. S.; Mate, C. M.; Somorjai, G. A. *Tribol. Lett.* **1995**, *1*, 233.
(25) Buffeteau, T.; Desbat, B.; Turlet, J. M. *Appl. Spectrosc.* **1991**, *45*, 380.
(26) Bain, C. D.; Whitesides, G. M. *J. Am. Chem. Soc.* **1988**, *110*, 6560.
(27) Gelius, U.; Heden, P. F.; Hedman, J.; Lindberg, B. J.; Manne, R.; Nordberg, R.; Nordling, C.; Siegbahn, K. *Phys. Scr.* **1970**, *2*, 70.

**Table 1. Percent Composition of Trifluoromethyl-Terminated Species in Mixed Hexadecanethiol Solutions and SAMs**

| solution (%)[a] | surface (%)[b] |
|---|---|
| 0 | 0 |
| 17 | 15 |
| 34 | 22 |
| 50 | 38 |
| 67 | 51 |
| 83 | 75 |
| 100 | 100 |

[a] Calculated from stoichiometries. [b] Determined by XPS.

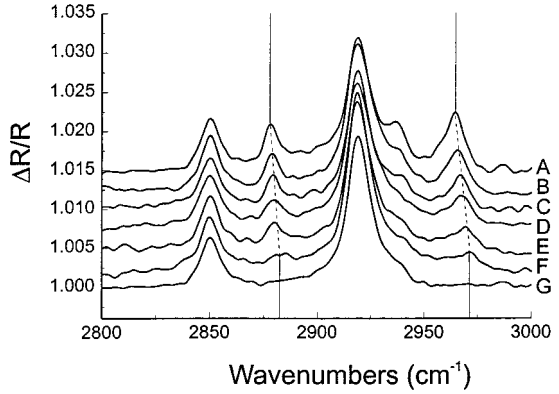


**Figure 2.** Polarization modulation infrared spectra of single component and mixed monolayers of hexadecanethiol and 16,16,16-trifluorohexadecanethiol as a function of film composition. The surface compositions of the respective films are as follows: (A) 100% hexadecanethiol and (B) 15%, (C) 22%, (D) 38%, (E) 51%, (F) 75%, and (G) 100% 16,16,16-trifluorohexadecanethiol. The dotted lines highlight the spectral shift of the symmetric and asymmetric methyl stretches upon incorporation of the larger $CF_3$ headgroup into the film.

(where the mole fraction equals 1.0); all other values were normalized to this ratio. The results of these calculations are listed in Table 1 and compare the solution and surface concentrations for the different mixed monolayers. Further reference to these mixed monolayers are made with respect to the percent composition within the monolayer film (surface composition).

The packing density and the degree of crystallinity of the mixed monolayers were evaluated through FTIR (specifically PM-IRRAS) measurements of the SAMs. Figure 2 compares the spectra obtained for the C−H stretching region of each of the mixed monolayers as well as the two single-component films. From these measurements, we first note the peak position and full-width half-maximum (fwhm) of the symmetric (2850 $cm^{-1}$) and asymmetric (2919 $cm^{-1}$) stretches of the methylene backbone units. Previous reports have documented both a shift in peak position as well as an increase in fwhm of these vibrational features with increasing molecular disorder within self-assembled films.[28] We observed no change in either the peak locations or fwhm for the mixed SAMs of various relative concentrations. Thus, we conclude that substitution (or doping) of the trifluoromethyl-terminated alkanethiol into a fully hydrogenated SAM fails to disrupt the packing and crystallinity. These observations are consistent with our previous report that **H1-B12** and **F1-B12** SAMs exhibit indistinct close-packed lattices.[8,9] Second, we note the intensity and peak positions of the symmetric (2878 $cm^{-1}$) and asymmetric (2964 $cm^{-1}$) $CH_3$ stretches. As expected, decreasing intensities of the

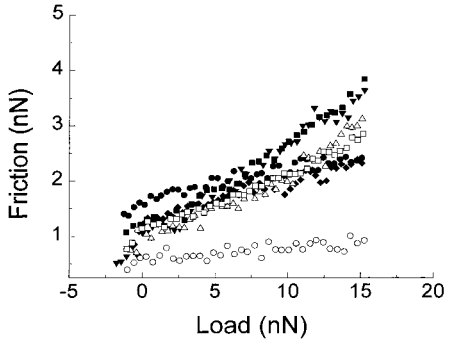


**Figure 3.** Frictional forces measured with AFM as a function of decreasing load for single-component and mixed monolayers composed of 100% hexadecanethiol (○), and 15% (□), 22% (△), 38% (●), 51% (◆), 75% (■), and 100% 16,16,16-trifluorohexadecanethiol (▼). The incorporation of even a small amount of the larger $CF_3$ terminal group leads to a substantial increase in the sliding friction.

methyl stretches are observed as the films are composed of increasing amounts of the trifluoromethyl-terminated monolayer. In addition, the symmetric and asymmetric stretches are observed to shift systematically to higher frequencies (4 $cm^{-1}$ shift, symmetric; 7 $cm^{-1}$ shift, asymmetric) with increasing surface compositions of the trifluoromethyl-terminated species. Similar shifts of terminal group frequencies have been observed in previous studies of self-assembled monolayers and attributed to the influence of nearest neighbors within the film system on the local environment of the terminal group.[29,30] The observed frequency shifts are consistent with the expected interactions of the methyl groups with the larger trifluoromethyl groups as the concentration of the fluorinated component is increased within the film.

The frictional properties of the mixed SAMs were investigated with atomic force microscopy. Two types of experiments were performed. For each monolayer of the series of different surface compositions, the film was imaged using lateral force microscopy. Over a wide range of areas (ca. 1−0.000025 $\mu m^2$) frictional images revealed no indication of phase separation of the methyl- and trifluoromethyl-terminated species. Previous studies have demonstrated that phase separation can be readily detected for systems composed of species with different frictional properties.[15,28] The approximate 3-fold difference in the frictional response of methyl- and trifluoromethyl-terminated monolayers ensures that sufficient image contrast would exist and reveal domains of the different components if they existed. In the absence of frictional contrast in the lateral force images, we conclude that the two components with identical backbone structures are uniformly mixed throughout the monolayer.

Finally, the frictional response of the mixed monolayers was evaluated from the dependence of friction on the applied total load as measured in a fashion similar to that previously reported.[24] Figure 3 provides a plot of friction vs decreasing load for each of the six mixed monolayers as well as for the two single-component monolayers formed from the methyl- and trifluoromethyl-terminated thiols. The data presented here were obtained from SAMs generated from **H1-B15** and **F1-B15**; similar results were obtained for SAMs generated from **H1-B12** and **F1-B12**. The relative percent of the **F1-B15** component in the SAMs varied as 0, 15, 22, 38, 51, 75, and 100 (see Table 1). As

(28) Hayes, W. A.; Kim, H.; Yue, X.; Perry, S. S.; Shannon, C. *Langmuir* **1997**, *13*, 2511.

(29) Allara, D. L.; Nuzzo, R. G. *Langmuir* **1985**, *1*, 52.

(30) Nuzzo, R. G.; Dubois, L. H.; Allara, D. L. *J. Am. Chem. Soc.* **1990**, *112*, 558.

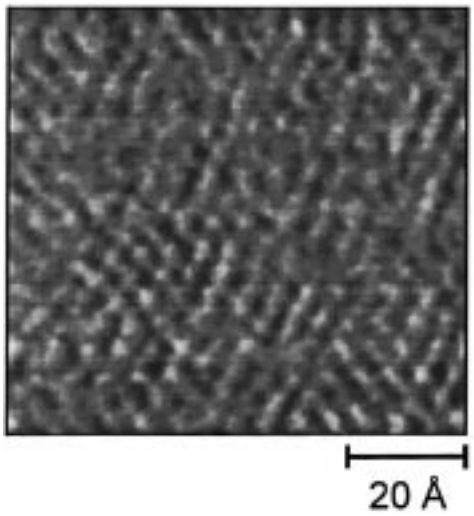


**Figure 4.** Lateral force image (120 Å x 120 Å) of an isopropyl-terminated SAM generated from 14-methyltetradecanethiol. The lattice resolution of this film was derived from the spatial dependence of the stick-slip behavior of the probe tip during movment across the surface of the film. The features of the image reveal a lattice spacing of 4.9 Å ± 0.2 Å, identical to the measured spacings of the methyl- and trifluoromethyl-terminated films.[8]

in our previous study,[8,9] we observed no substantial differences in the pull-off force measured during sliding, which suggests no substantial differences in adhesive forces between the AFM tip and the various SAMs. Furthermore, as seen in Figure 3, the introduction of the trifluoromethyl-terminated component leads to an increase in the frictional response, even at the lowest compositions. Perhaps due to slight variations in the film response or sample alignment within a given sets of measurements, no systematic correlation between the trifluoromethyl composition and the frictional response could be observed. Again, it is important to note that the same cantilever/tip assembly was used for all of these measurements and that no substantial wear of the tip occurred during the course of the measurements. The spread in the frictional data for the different mixed monolayer films is representative of the variation encountered in these molecular-scale measurements.

**Isopropyl-Terminated Alkanethiols.** We further explored the issue of steric contributions to the frictional behavior of well-formed organic monolayers[8,9] by examining isopropyl-terminated SAMs (**IP** SAMs), which, like trifluoromethyl-terminated SAMs (**F1** SAMs), expose a larger tail group than methyl-terminated SAMs (**H1** SAMs). Literature studies calculate, for example, that the relative van der Waals cross sections of the three tail groups increase in the following order: methyl (13 Å$^2$), isopropyl (19 Å$^2$), and trifluoromethyl (23 Å$^2$).[31] Despite the relatively large size of the **F1** tail group, we observed in recent studies that it was accommodated into the close-packed ($\sqrt{3} \times \sqrt{3}$)R30° overlayer structure characteristic of **H1** SAMs without changing the dimensions of the unit cell.[8]

We generated SAMs on Au(111) by exposure of the freshly prepared gold to solutions containing the **IP-B12** and **IP-B13** alkanethiols. Lateral force images of the SAMs formed by this procedure show well ordered monolayers on the molecular scale (Figure 4) and are comparable to lateral force images previously reported for the **H1-B12** and **F1-B12** monolayers.[8] The contrast in these images

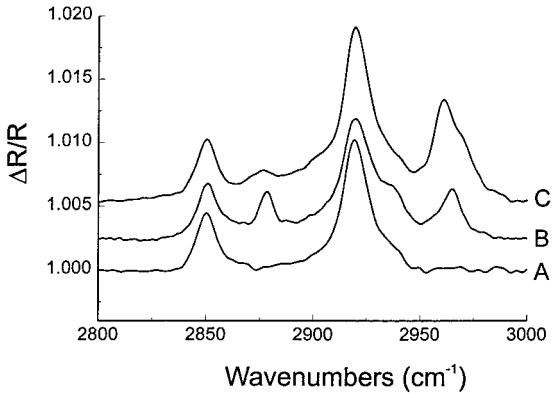


**Figure 5.** Polarization modulation infrared spectra in the CH stretching region for SAMs composed of (A) **IP-B13**, (B) **H1-B13**, and (C) **F1-B13**. The similarities in the peak locations and widths for the symmetric (2850 cm$^{-1}$) and asymmetric (2919 cm$^{-1}$) methylene stretches indicate no differences in the packing density or order of the films having larger terminal groups.

arises from the stick−slip motion of the tip as it is rastered across the surface of the monolayer.[32] Although the features fail to represent true molecular resolution, the variation in frictional intensity is representative of the molecular spacing of the molecules within the monolayer. An analysis of this spacing reveals a value of 4.9 ± 0.2 Å between nearest neighbors within the film; this value is indistinct from that observed for **H1** SAMs. We attribute the similarity in molecular spacing for **H1** and **IP** SAMs to the packing energy of the two films, which arises predominantly from their similar backbone structures. Similarities in the packing energies of the films with different terminal groups are again supported by PM-IRRAS data (Figure 5). In these spectra, the stretching frequencies of the terminal groups systematically vary from the symmetric and asymmetric stretches of the methyl group for the alkanethiol films to the doublets observed in the methyl region for the isopropyl-terminated film to the absence of features in this region for the trifluoromethyl-terminated films. However, for each of the films, the symmetric (2850 cm$^{-1}$) and asymmetric (2919 cm$^{-1}$) methylene stretches remain constant in peak location and fwhm. This invariance strongly suggests that the incorporation of the larger terminal groups fail to perturb the nature of the packing of the identical backbone structures.

Figure 6 compares the frictional properties of the **IP-B13** monolayer to those of the **H1-B13** and **F1-B13** films that possess similar backbone structures; a similar response was measured for the **B12** series. The data were measured as a function of decreasing load; similar frictional responses were obtained as a function of increasing load. These data show that **IP** monolayers exhibit a frictional behavior intermediate to that of the **H1** and **F1** monolayers. In light of the similarity in chemical composition of the **IP** and **H1** monolayers (i.e., they consist of only carbon and hydrogen), we attribute the observed frictional difference between these two films to the difference in size of the tail groups.[8,9] This proposal is further consistent with the observed correlation between the frictional responses and the relative sizes of the **H1**, **IP**, and **F1** moieties.

## Discussion

In our previous investigation, we observed that the frictional response of the **F1-B12** SAM was approximately

(31) Seebach, D. *Angew. Chem., Int. Ed. Engl.* **1990**, *29*, 1320.

(32) Carpick, R. W.; Salmeron, M. *Chem. Rev.* **1997**, *97*, 1163.

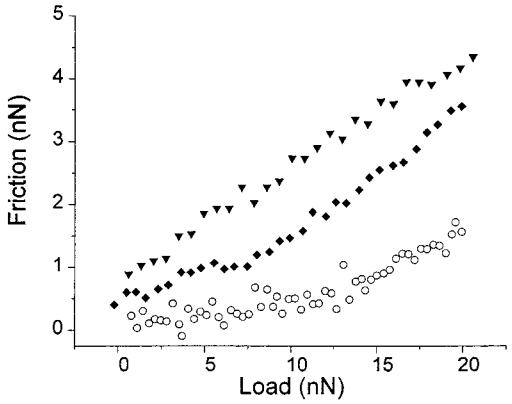


**Figure 6.** Frictional forces measured with AFM as a function of decreasing load for SAMs composed of **IP-B13** (◆), **H1-B13** (○), and **F1-B13** (▼). The film composed of the intermediate sized isopropyl terminal group exhibits a frictional response intermediate to that of the methyl- and trifluoromethyl-terminated films.

three times higher than that of the **H1-B12** SAM.[8,9] In light of indistinguishable differences in the lattice spacing of the two films, we attributed the surprisingly large increase in friction upon substitution of the $CH_3$ terminal group with the $CF_3$ terminal group to two potential factors: (1) intramolecular energetic barriers to rotation of the bulkier $CF_3$ terminal group and (2) long-range intermolecular steric interactions within the plane of the bulkier $CF_3$ terminal groups. The data obtained in the present study provide further experimental support for this model.

To evaluate the steric contributions to the frictional response, we first examined mixed two-component monolayers formed from the "low" friction methyl-terminated alkanethiols and the "high" friction trifluoromethyl-terminated alkanethiols; a critical element of this study was again the presence of identical backbone structures in the films. We chose to study mixed films in an effort to disentangle steric contributions from potential chemical and/or adhesive interactions. We reasoned that a greater chemical/adhesive interaction between the tip and the $CF_3$ terminal groups would give rise to a direct (if not linear) relation between the increase in friction and the relative surface concentration of the $CF_3$ groups. The frictional data in Figure 3, however, indicate a nonlinear relationship: at all applied loads, the introduction of even small concentrations of the $CF_3$ component gives rise to a substantial increase in the frictional response compared to that of the single-component $CH_3$-terminated film.

While arguing against the participation of chemical/adhesive interactions, the data in Figure 3 provide support for a mechanism of frictional response that is based on intermolecular steric interactions. As illustrated in Figure 7, this type of mechanism need not scale directly with the number of larger tail groups incorporated into a well-ordered film. In Figure 7, the filled circles represent larger tail groups at low concentrations (ca. 10%) in a hexagonal close-packed structure. Although we are not suggesting that the trifluoromethyl-terminated molecules form an ordered superstructure, the schematic, nevertheless, illustrates how the presence of a low number of larger tail groups might influence the intermolecular interactions in a substantial portion (ca. 75%) of the film. In our proposed mechanism, the introduction of the larger tail groups gives rise to additional steric barriers to the motion of the nearest neighbors. In the process of overcoming these barriers, the dissipation of interfacial energy during

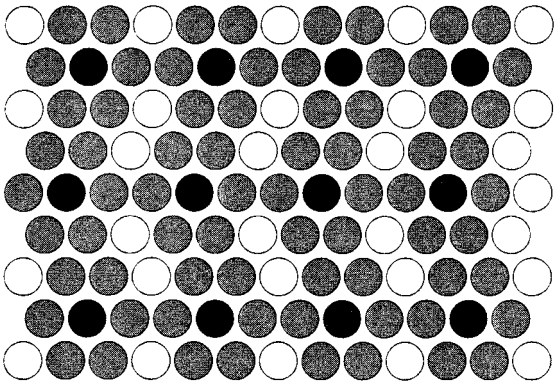

**Figure 7.** Schematic representation of the degree of intermolecular influence in highly dispersed mixed SAMs. In practice, the mixed films likely form no ordered array of the coadsorbates. Filled circles represent the trifluoromethyl-terminal groups at a surface concentration of ~10%, while shaded circles represent neighboring methyl groups sterically influenced by their proximity to the larger terminal groups. This model rationalizes the large observed increase in the frictional response of mixed monolayers composed of relatively small amounts of the trifluoromethyl-terminated species.

sliding is manifested as an increase in the frictional response.[8] In this model, the intermolecular motions of the nearest neighbors (shaded circles) would contribute to the frictional increase as well as those of the larger tail groups. Consequently, the increase in friction would be proportional to the increase in steric interactions rather than the number of larger tail groups. We admit that the perfectly ordered array of larger tail groups shown in Figure 7 represents an upper limit to the degree of influence; in the absence of phase separation, however, we still anticipate a substantial impact even at low concentrations of $CF_3$ moieties.

The frictional response of the isopropyl-terminated SAMs further supports our proposed model that steric barriers to intermolecular motion give rise to a increased frictional response in well-ordered organic thin films. As noted above, an isopropyl group possesses a larger van der Waals diameter than a methyl group.[31] As seen in Figure 6, the complete substitution of an isopropyl terminal group for a terminal methyl group produces an approximate 2-fold increase in the frictional response of the SAMs. This increase in friction arises solely from the introduction of the isopropyl moieties, as the local spacing and order of the film structure remains unchanged (Figures 4 and 5). Furthermore, since both the methyl and the isopropyl groups are hydrocarbon species, it seems untenable that there would exist differences in chemical/adhesive interactions between the probe tip and the tail groups. We therefore conclude that the enhanced frictional response observed for the isopropyl-terminated SAMs arises from additional steric barriers to molecular motion within the plane of the terminal isopropyl groups. The observed enhancement for the isopropyl-terminated films is entirely analogous to that observed for the trifluoromethyl-terminated films.[8,9] In addition, the observed magnitude of frictional enhancement is consistent with the relative sizes of the tail groups (vide supra).

## Conclusions

Through quantitative measurements of the interfacial forces between an AFM tip and systematically well-defined monolayers on atomically flat surfaces, we have investigated the molecular factors that influence the frictional properties of purely hydrocarbon and partially fluorinated

organic thin films. These studies demonstrate that the frictional properties are highly correlated with the molecular structure/composition of the self-assembled films. We find, for example, that the introduction of small percentages of $CF_3$ termini into $CH_3$-terminated SAMs leads to a substantial increase in the frictional response. Furthermore, we find that the magnitudes of the frictional response correlate directly with the size of the terminal groups: $CH_3 < CH(CH_3)_2 < CF_3$. These results are consistent with a model in which long-range intermolecular steric interactions among bulky tail groups are the major contributing factors to the enhancement in frictional properties. These findings provide further support for our earlier proposal that fluorinated SAMs exhibit higher frictional properties due to a "tighter" intermolecular packing at the interface.[8,9] This "tighter" packing arises from the placement of relatively large terminal groups (e.g., $CH(CH_3)_2$ and $CF_3$) into the close-packed ($\sqrt{3} \times \sqrt{3}$)R30° lattice that is normally occupied by smaller methyl groups. This "tighter" packing gives rise to increased steric interactions between adjacent terminal groups in the outermost plane of the film. To overcome the consequent increased steric barriers (translational and/or rotational), more energy is imparted to the film during sliding, which manifests itself as an enhanced frictional response.

**Acknowledgment.** Financial support was provided by the National Science Foundation (DMR-9700662). Acknowledgment is made to the donors of the Petroleum Research Fund, administered by the American Chemical Society, for partial support of this research (ACS-PRF# 30614-G5). We thank Mr. Arif Rahman for assistance with the synthesis of the isopropyl-terminated alkanethiols. This work made use of MRSEC/TCSUH Shared Experimental Facilities supported by the National Science Foundation under Award Number DMR-9632667 and the Texas Center for Superconductivity at the University of Houston.

LA981497H